Modeling of Photo Voltaic Arrays with Soft Switching Converter Design and Simulation for Maximum Power Point Tracking

N.SenthilMurugan
Assistant Professor
Dept. of Electrical & Electronics Engineering
Sri Venkateswara College of Engineering, Sriperumbudur, Tamilnadu, India.

C.Sharmeela
Assistant Professor
Dept. of Electrical & Electronics Engineering
A.C. Tech, Anna University, Guindy Chennai, Tamilnadu, India.

K.Saravanan
Associate Professor
Dept. of Electrical & Electronics Engineering
Arupadai Veedu Institute of Technology, Paiyanoor, Tamilnadu, India.

ABSTRACT
This paper deals with the determination of the nonlinear I–V parameters of the equation by adjusting the curve at three points: open circuit, maximum power, and short circuit. Given these three points, which are provided by all commercial array datasheets, the method finds the best current- voltage (I–V) equation for the Single-diode photovoltaic (PV) model including the effect of the series and parallel resistances and confirms the maximum power of the model matches with the maximum power of the real array. The novel soft switching converter is designed for maximum power point tracking (MPPT). The mathematical model of the PV device may be useful in the study of the dynamic analysis of converters, in the study of MPP tracking (MPPT) algorithms. The converter aims to get the regulated output voltage from photovoltaic (PV) arrays with low switching loss and conduction loss and efficiency of more than 92% can be easily achieved.

General Terms
Photo voltaic array modeling and MATLAB simulation, soft switching converter topology PSpice computer simulation for solar hybrid applications.

Keywords
Zero Voltage Switching (ZVS), Zero Current Switching (ZCS), and Maximum power point tracking (MPPT).

1. INTRODUCTION
In late years, the problem of energy crunch is more and more aggravating. Very much exploitation and research for new power energy are preceded around the world. In particular, the solar energy attracts lots of attention. In recent years, the development of power semiconductor technology results in easier conversion between AC and DC. Therefore, the use of solar energy is emphasized increasingly and regarded as an important resource of power energy in the next century.[1] The solar modules have a long lifetime (20 years or more) and their best production efficiency is approaching 20%. Solar energy can be utilized in two ways, solar heating/cooling and solar electricity. Some appliances can be connected directly because they work on dc at the system voltage. Solar arrays were developed for power satellites in the space program. In high power applications, parallel connected converters are often used to provide electrical power. As the power supplied by solar arrays depends upon the insolation, temperature and array voltage, it's required to draw maximum power from solar array. A PV system directly converts sunlight into electricity. The basic device of a PV system is the PV cell. Cells may be grouped to form panels or arrays. The voltage and current available at the terminals of a PV device may directly feed small loads such as lighting systems and DC motors. More sophisticated applications require electronic converters to process the electricity from the PV device. These converters may be used to regulate the voltage and current at the load, to control the power flow in grid-connected systems, and mainly to track the maximum power point (MPP) of the device. In order to study electronic converters for PV systems, one first needs to know-how model the PV device that is attached to the converter. PV devices present a nonlinear I–V characteristic with several parameters that need to be adjusted from experimental data of practical devices. The mathematical model of the PV device may be useful in the study of the dynamic analysis of converters, in the study of MPP tracking (MPPT) algorithms. A set of connected cells form a panel. Panels are generally composed of series cells in order to obtain large output voltages. Panels with large output currents are achieved by increasing the surface area of the cells or by connecting cells in parallel. A PV array may be either a panel or a set of panels connected in series or parallel to form large PV systems. The PV module with all necessary variables and constraints of the governing equations are considered and the tracking efficiencies are confirmed by simulations and experimental results. Fig.1 shows the solar array I-V characteristics and the load curve, together with constant power curves ($P = VI = const$). It is observed that the delivered output power, which is represented by the operating point 1, is significantly smaller than the maximum output power, which is represented by point 2. In order to ensure a maximum power transfer, DC/DC converters are used to adjust the voltage at the load to the value of $Vr = \sqrt{(Pm.R)}$, r – equivalent resistance of the load. This paper presents a cost-effect controller system for 1kW to 5kW PV system with low DC voltage input (18V DC or 48V DC) and high output DC voltage (350V DC). The converter

module is to regulate output voltage of PV cells feeding battery / grid load under dynamic conditions.

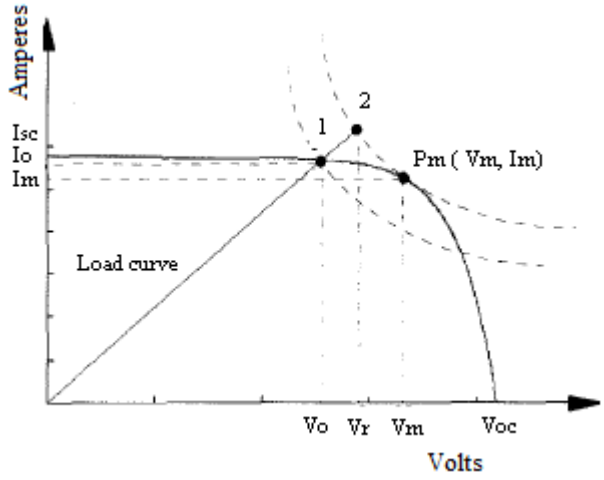

Fig. 1 The operation of the MPPT

Energy conservation has become a priority nowadays. Table. 1 give, using PV systems how $C0_2$ emissions reduced drastically. Over a five year operating period, corresponding approximately to the life duration of the Ni-Cd battery and of the gen set in such an array application, the reduction in the $C0_2$ emission for a 2 kW mobile site with this PV power system will be higher than 200 tons. [2] This 200 tons should be compared with about only 2.7 tons of equivalent $C0_2$. The addition of a wind turbine or possibly solar panels will emphasize this reduction in $C0_2$ with an increase in cycling time.

Table. 1 Example of CO_2 savings with PV system and generator

Operational Details	**2.5 KW System**	**6 KW System**	**12 KW System**	**24 KW System**
Daily Generator Operation	8.25h	9h	9h	11.75h
Daily Battery Operation	15.75h	15h	15h	12.25h
CO_2 savings Per year	58 Tons	56 Tons	58 Tons	42 Tons

2. SOFT SWITCHING CONVERTER OPERATION

In this paper, a power generation system using soft switching technique is proposed as shown in Fig 2. The proposed system consists of a ZVS-ZCS boost converter, a half-bridge LLC resonant converter and transformer. However, since the transformer has normally large air-gap, while the leakage inductance increases and magnetization inductance decreases. This causes low power conversion efficiency. To overcome such problems, a series resonant converter is widely used [3] [4]. However, the series resonant converter for the power supply generally operates with higher switching frequency than resonant frequency to achieve soft switching under continuous resonant current mode. In this case, the main switches can achieve zero voltage switching (ZVS), but it has disadvantage that the secondary side diode converter cannot achieve zero current switching. Furthermore, due to the higher switching frequency operation than resonant frequency, it has low voltage gain and high power loss since a large primary side circulating current flows [5]. Since the proposed power supply using LLC converter operates with lower switching frequency than the resonant frequency, it can achieve high voltage gain, which, in turn, offers low turns ratio for the transformer and high efficiency due to discontinuous resonant current.

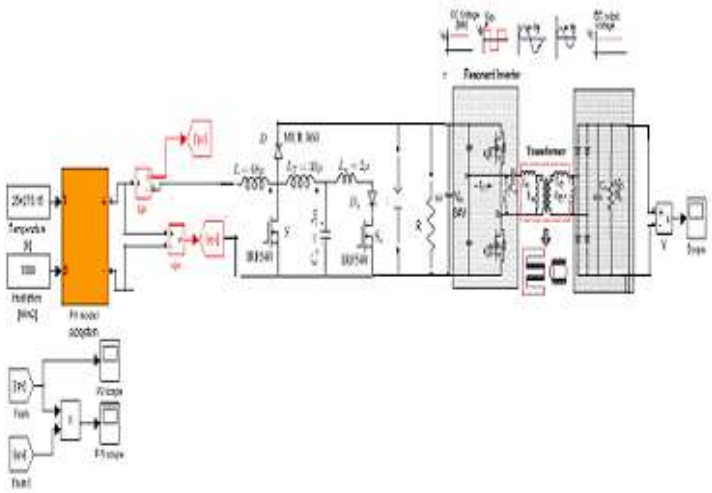

Fig. 2 Simplified circuit of proposed PV system with ZVS-ZCS boost converter

Figure 2 gives the simplified circuit of the proposed PV system with ZVS-ZCS boost converter to track the maximum power and deliver the load finally. The PV model subsystem is constructed by all governing mathematical modeling equations and with different possible inputs like temperature, insolation etc,.

Table. 2 give the specification of the converter with resonant action for low switching loss and conduction loss which is used for MPPT tracking

Table. 2 Specification of Half bridge converter

Input voltage(V_{in})	12V DC	Transformer turn ratio(N)	n1/n2 17/5=3.4
Output voltage(V_o)	350V DC	Equivalent leakage inductance(L_{eq})	22.54nH
Output power(P_o)	1000W	Resonant capacitor(C)	50nF
Resonant frequency(f_r)	150kHz	Magnetic inductance(L_m)	51.95nH
Switching frequency(f_s)	100-150kHz	Primary side leakage inductance(L_{l1})	19.74nH
Coupling coefficient (k)	0.828	Secondary side leakage inductance(L_{l2})	25.6nH

3. POWER MODULE IN PARALLEL

The DC-DC boost converter stage, used to convert 18V DC or 48V DC to 350 DC, is designed as 1kW module that can dynamically adjust its output current in terms of load current. In this way, 3kW and 5kW system can be derived from the 1kW system with the parallel operation of multi independent modules in 1kW. These multiple independent power modules can be paralleled such that each module supplies only its [6] proportionate share to total-load current. This sharing is accomplished by controlling each module's power stage with a command generated from a voltage feedback amplifier whose reference can be independently adjusted in response to a common-share-bus voltage. By monitoring the current from each module, the current share bus circuitry determines which paralleled module would normally have the highest output current and with the designation of this unit as the master, adjusts all the other modules to increase their output current to within 2.5% of that of the master. The 1kW DC-DC stage with load sharing controller UC3907 and PWM controller SG3525 is shown in Fig.3

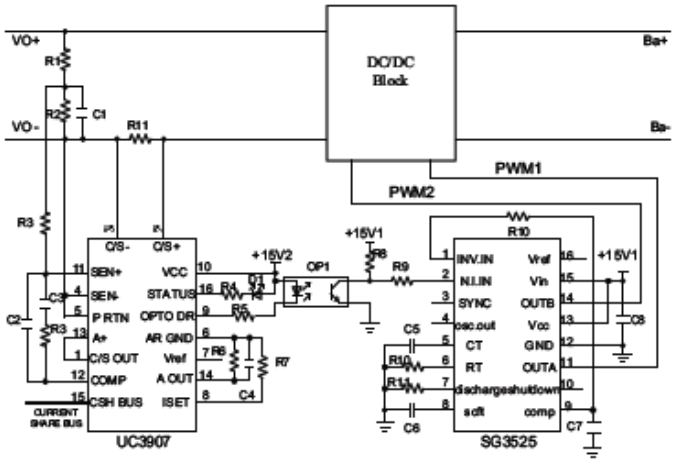

Fig. 3 PWM dive and current sharing control

4. MODELING OF PV DEVICES

4.1. Ideal PV Cell

Fig. 4 shows the equivalent circuit of the ideal PV cell. The basic equation from the theory of semiconductors [7] that mathematically describes the *I–V* characteristic of the ideal PV cell is

$$I = I_{\mathrm{pv,cell}} - \underbrace{I_{0,\mathrm{cell}}\left[\exp\left(\frac{qV}{akT}\right) - 1\right]}_{I_d} \quad \text{--------- (1)}$$

where *I*pv, cell is the current generated by the incident light (it is directly proportional to the Sun irradiation), *I*d is the Shockley diode equation, *I*0, cell is the reverse saturation or leakage current of the diode, *q* is the electron charge (1.60217646 × 10−19 C), *k* is the Boltzmann constant (1.3806503 × 10−23 J/K), *T* (in Kelvin) is the temperature of the *p–n* junction, and α is the diode ideality constant. Fig. 5 shows the *I–V* curve originated from (1). The basic equation (1) of the elementary PV cell does not represent the *I–V* characteristic of a practical PV array.

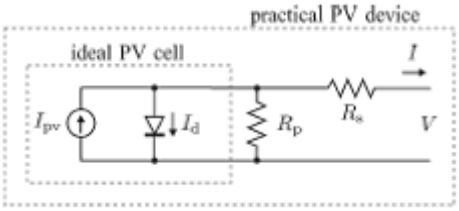

Fig. 4 Single diode model of the theoretical PV cell and equivalent circuit of a practical device including the series and parallel resistances

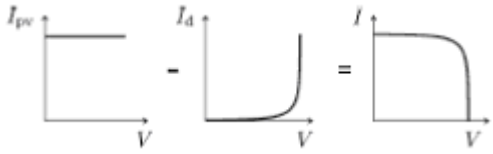

Fig. 5 Characteristic I-V curve of the PV cell. The net cell current I is composed of the light generated current Ipv and the diode current Id.

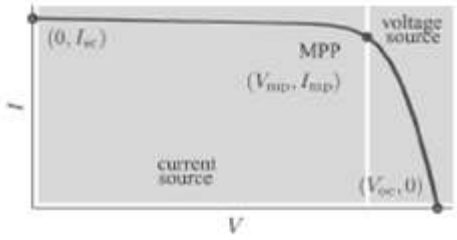

Fig. 6 Characteristic I-V curve of a practical device and the three remarkable points: short circuit (0, Isc), MPP (Vmp, Imp) and the open circuit (Voc, 0)

Practical array requires the inclusion of additional parameters to the basic equation,

$$I = I_{\mathrm{pv}} - I_0 \left[\exp\left(\frac{V + R_{\mathrm{s}} I}{V_{\mathrm{t}} a} \right) - 1 \right] - \frac{V + R_{\mathrm{s}} I}{R_{\mathrm{p}}}$$

--------- (2)

arrays are composed of several connected PV cells and the observation of the characteristics at the terminals of the PV where *I*pv and *I*0 are the photovoltaic (PV) and saturation currents, respectively, of the array and *V*t = *N*s*kT/q* is the thermal voltage of the array with *N*s cells connected in series. Cells connected in parallel increase the current and cells connected in series provide greater output voltages. If the array is composed of *N*p parallel connections of cells the PV and saturation currents may be expressed as *I*pv = *I*pv, cellNp, *I*0 = *I*0, cellNp. In (2), *R*s is the equivalent series resistance of the array and *R*p is the equivalent parallel resistance. This equation originates the *I–V* curve in Fig. 6, where three remarkable points are highlighted: short circuit (0, *I*sc), MPP (*V*mp, *I*mp), and open circuit (*V*oc, 0) and resultant maximum power developed Pm (given in Table 3)

Table. 3 Effect of change in solar irradiation

G	Isc	Voc	Power
100	1.6	0.89	0500
200	3.3	0.92	1050
300	5.0	1.00	1800
500	8.0	1.00	3000
1000	16.3	1.00	6000
1500	24.5	1.00	9000
1900	31.5	1.00	11000
2000	33.0	1.00	11900

Table. 3 give the effect of change in solar radiation with respect to the open circuit voltage, short circuit current and resultant power developed

4.2. Modeling the PV array

Assumption / Drawback of the proposed work so far by the different authors is that parallel resistance in single diode model is neglected and series resistances are assumed to be low [8] [9]. Moreover *I*sc ≈ *I*pv are considered but short circuit current and PV cell current are not same practically where as in our proposed work we have considered both resistances and framed the equation and cell currents are considered practically. The I–V characteristic of the PV device shown in Fig. 6 depends on the internal characteristics of the device (*R*s, Rp) and on external influences such as irradiation level and temperature. The assumption *I*sc ≈ *I*pv is generally used in the modeling of PV devices because in practical devices the series resistance is low and the parallel resistance is high. The light-generated current of the PV cell depends linearly on the solar irradiation and is also influenced by the temperature according to the following equation

$$I_{\mathrm{pv}} = (I_{\mathrm{pv,n}} + K_{\mathrm{I}} \Delta_{\mathrm{T}}) \frac{G}{G_{\mathrm{n}}}$$

--------- (3)

where *I*pv, n (in amperes) is the light-generated current at the nominal condition (usually 25 ◦C and 1000 W/m2), ΔT = T − *T*n (*T* and *T*n being the actual and nominal temperatures [in Kelvin], respectively), *G* (watts per square meters) is the irradiation on the device surface, and *G*n is the nominal irradiation. The diode saturation current *I*0 and its dependence on the temperature may be expressed by as shown [10].

$$I_0 = I_{0,\mathrm{n}} \left(\frac{T_{\mathrm{n}}}{T} \right)^3 \exp\left[\frac{q E_{\mathrm{g}}}{ak} \left(\frac{1}{T_{\mathrm{n}}} - \frac{1}{T} \right) \right]$$

--------- (4)

where *E*g is the bandgap energy of the semiconductor (*E*g = 1.12 eV for the polycrystalline Si at 25 ◦C [11] and *I*0, n is the nominal saturation current.

$$I_{0,\mathrm{n}} = \frac{I_{\mathrm{sc,n}}}{\exp(V_{\mathrm{oc,n}} / a V_{\mathrm{t,n}}) - 1}$$

--------- (5)

with *V*t, n being the thermal voltage of *N*s series-connected cells at the nominal temperature *T*n . The value of the diode constant α may be arbitrarily chosen. Usually, 1 ≤ α ≤ 1.5 and the choice depends on other parameters of the *I–V* model. Some values for α are found based on empirical analyses. As α expresses the degree of ideality of the diode and it is totally empirical, any initial value of α can be chosen in order to adjust the model. The value of α can be later modified in order to improve the model fitting, if necessary. This constant affects the curvature of the I–V curve and varying α can slightly improve the model accuracy. The PV model described in the equation (5) can be improved by,

$$I_0 = \frac{I_{\mathrm{sc,n}} + K_{\mathrm{I}} \Delta_{\mathrm{T}}}{\exp((V_{\mathrm{oc,n}} + K_{\mathrm{V}} \Delta_{\mathrm{T}}) / a V_{\mathrm{t}}) - 1}$$

--------- (6)

This modification aims to match the open-circuit voltages of the model with the experimental data for a very large range of temperatures.

5. MATLAB IMPLEMENTATION OF MODEL EQUATIONS

The PV module subsystem is considered based on the mathematical model and the governing empirical equations for different voltage and current variables including resistances of the single diode model.

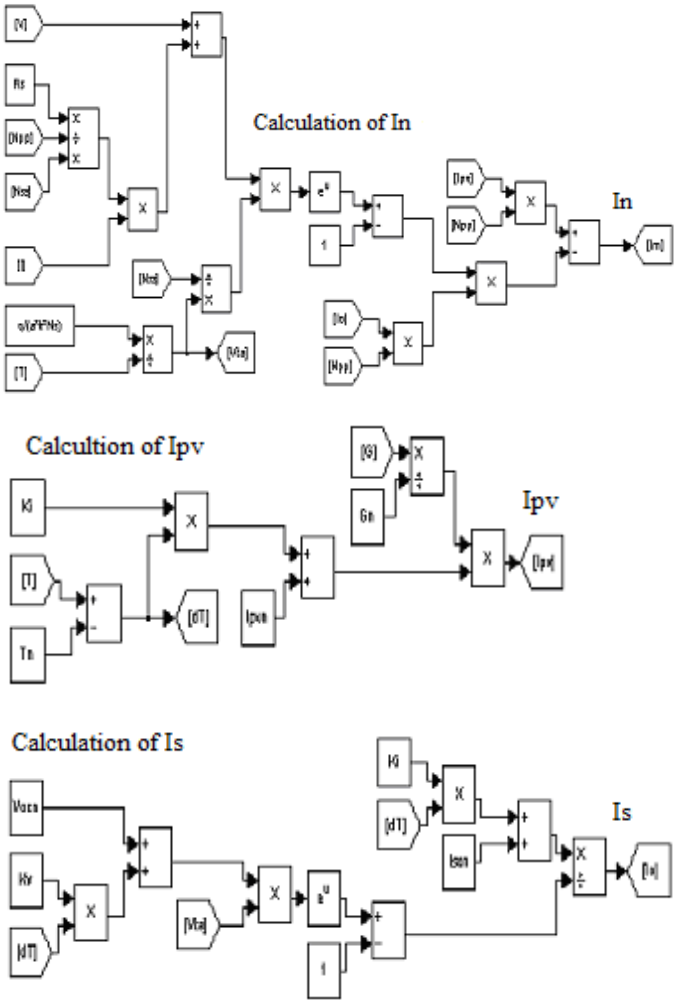

Fig. 7 Modeling blocks in MATLAB

6. MPPT CONTROL OF PV SYSTEM

The basic block diagram of the MPPT control is shown in Fig. 8. The proposed control consists of two loops, the maximum power point tracking loop is used to set a corresponding 'Vref' to the charger input, the regulating voltage loop is used to regulate the solar array output voltage according to 'Vref' which is set in the MPPT loop.

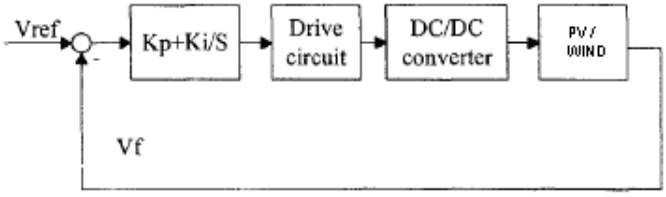

Fig.8 Basic block diagram of the control loop

7. PV ARRAY OUTPUT CHARACTERISTICS -

7.1 Matlab simulation results

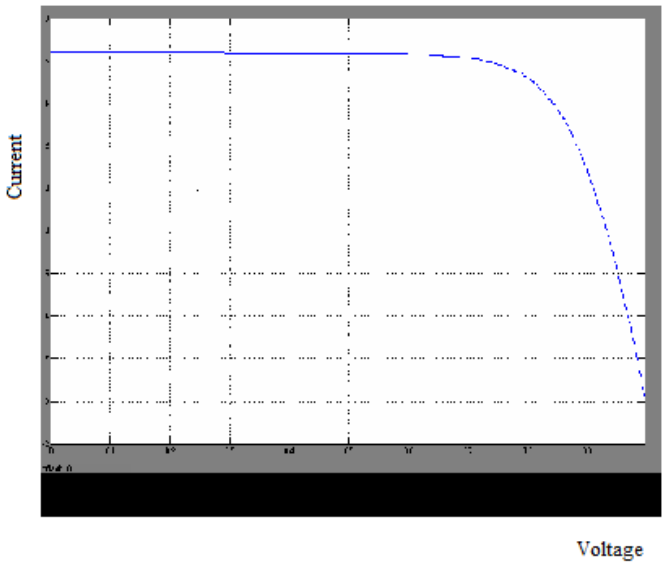

Fig. 9 PV array V-I characteristics

Figure 9 and 10 gives the PV array V-I characteristics and P-V curve respectively. Both the simulated characteristics are similar to the ideal characteristics of the PV array cells (refer Fig. 1), hence confirming the positive result of our proposed work.

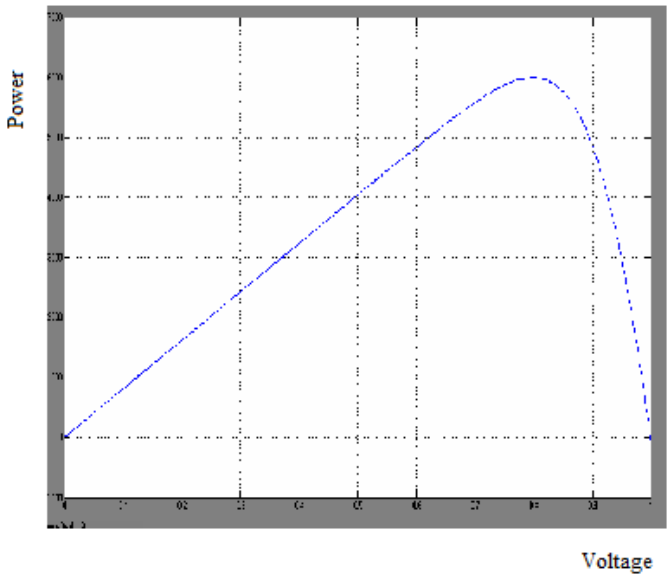

Fig 10 P-V curve

8. SIMULATION OF CONVERTER

The Figure 11 represents the simulated boost converter with coupled inductor. Simulated results of the 1KW, 150 kHz boost converter with auxiliary switch are presented.

The simulated system consists of a half-bridge LLC resonant converter with typical resistance, inductance and capacitance values for resonant action to confirm the maximum efficiency with very low switching and conduction losses.

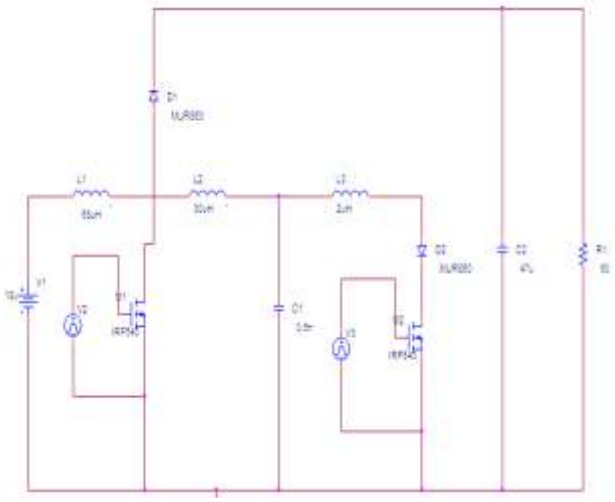

Fig. 11 Simulated boost converters with coupled inductor

9. INPUT/OUTPUT WAVEFORMS – SIMULATION RESULTS

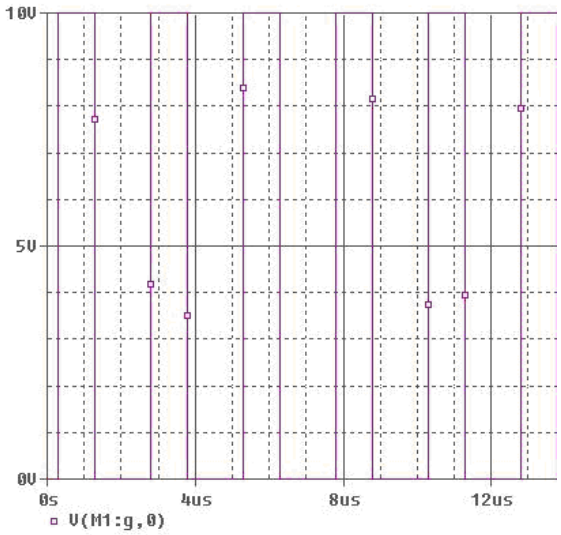

Fig.12 Gate pulse for main switch

Figure 12 show the pulse driving the main switch S. The main switch is turned on with a delay of 0.3 µs after the auxiliary switch is turned on and Figure 13 gives the resonant inductor current waveform with gate pulse of auxiliary switch.

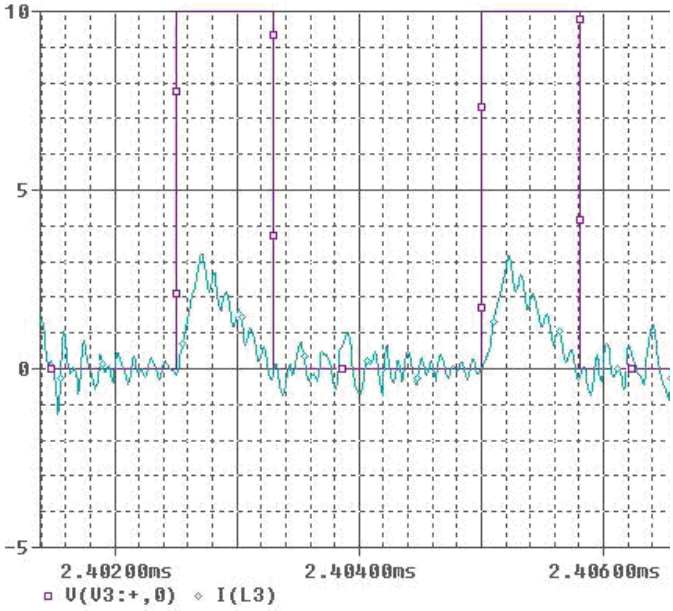

Fig. 13 Resonant inductor current and gate pulse of auxiliary switch

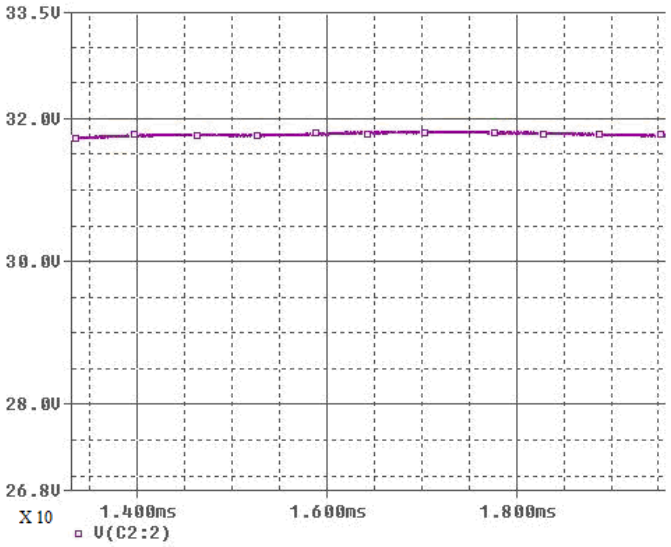

Fig. 14 System's regulated constant output voltage

From Figure 14 we infer that the constant dc output voltage is obtained as a result of simulation also from Figure 15 the maximum efficiency of the proposed PV converter system approaching above the value of 92% due to computation of various losses like diode, converter and inverter conduction losses and of course the soft switching operation achieved by the proposed novel boost resonant converter.

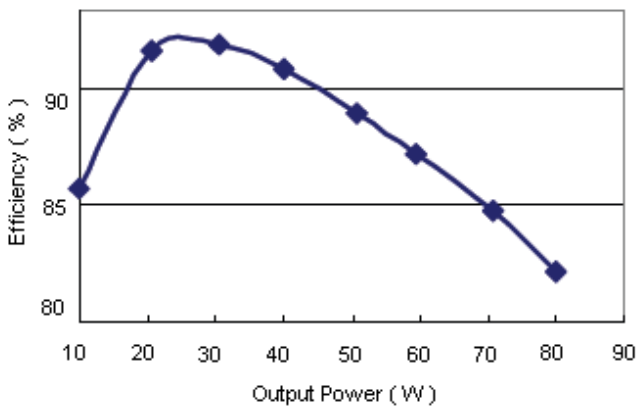

Fig. 15 ZVS action and efficiency characteristics of the proposed PV converter system.

10. CONCLUSION

In our proposed work of modeling the PV array, we have considered both series and parallel resistances and framed the equation and solar cell currents are considered practically which overcomes the drawback of the existing work where parallel resistance in single diode model is neglected and series resistances are assumed to be low and Isc ≈ Ipv are considered same but short circuit current and PV cell current are not practically equivalent. The design of novel soft switching converter with maximum power point tracking algorithm for PV systems to achieve high efficiency and to deliver maximum power to the load was explained. An auxiliary switch dc–dc boost converter using coupled inductor that achieves soft switching for both the main and auxiliary switches without increasing the main device current/voltage rating. Simulation results are presented for a 1KW, 150 kHz boost converter with excellent performance (efficiencies over 92% for ZVS-ZCS converters).

11. REFERENCES

[1] Youjie Ma, Deshu Cheng and Xuesung Zhou, 2009. Hybrid Modeling & Simulation for boost converter in Photo Voltaic system. In Proceedings of the IEEE Computer Society International Conference on Information and Computer Science, (January 2009), 85-87.

[2] .S.M.Mousavi, S.H Fathi, 2009. Energy Management of Wind/PV and battery hybrid system, In Proceedings of the IEEE Industrial Electronics, (August 2009), 630- 633.

[3] Joel Brunarie, George Myerscough, 2008. Delivering Cost Savings & Environmental Benefits with hybrid Power, In Proceedings of the IEEE Transactions on Industrial Electronics, (January 2008), 1203-1212.

[4] M. Z. Youssef, H. Pinheiro, and Praveen K. Jain, 2003. Analysis and Modeling of a Self-Sustained OscillationAnalytical Technique, In Proceedings of the IEEE International Energy and Telecommunications Conference, INTELEC, (October. 2003), 282-289

[5]. Laszlo Huber, Kevin Hsu and Milan M. Jovanovic, 2006. 1.8-MHz, 48-V resonant VRM: Analysis, Design and Performance Evaluation, In Proceedings of the IEEE transactions on Power Electronics, (January 2006) 79-88.

[6]. M.Lopez, D.Morales, J.C Vannier, and D.Sadar nac, 2007. Influence of Power Converter losses evaluation in sizing of a Hybrid Energy system. In Proceedings of the IEEE Transactions on Power Electronics, (March 2007), 249-254.

[7]. W. Xiao, W. G. Dunford, and A. Capel, 2004. A novel modeling method for photovoltaic cells. In Proceedings of the IEEE 35th Annual Power Electronics Conference (PESC), 1950–1956.

[8]. G.Walker, 2001.Evaluating MPPT converter topologies using a matlab PV model. Journal of EEE. Engineering., Australia, 45–55.

[9]. M. Veerachary, 2006. PSIM circuit-oriented simulator model for the nonlinear photovoltaic sources. In Proceedings of the IEEE Transactions on Aerospace Electron System, (April. 2006) 735–740.

[10]. W. De Soto, S.A.Klein, and W. A. Beckman, 2006. Improvement validation of a model for photovoltaic array performance, Solar Energy, (January 2006), 78-88.

[11]. Q. Kou, S. A. Klein, and W. A. Beckman, 1998. A method for estimating the long-term performance of direct-coupled PV pumping systems, SolarEnergy, (Sep. 1998) 33-40.